ACS APPLIED MATERIALS & INTERFACES

www.acsami.org

Research Article

Scalable Flexible Phase Change Materials with a Swollen Polymer Network Structure for Thermal Energy Storage

Fang Wei, Chang-Ping Feng,* Jie Yang, Lu-Yao Yang, Lu Bai, Rui-Ying Bao, Zheng-Ying Liu, Ming-Bo Yang, and Wei Yang*

Cite This: *ACS Appl. Mater. Interfaces* 2021, 13, 59364–59372

Read Online

ACCESS | Metrics & More | Article Recommendations | Supporting Information

ABSTRACT: 3D porous structural materials are proved to be enticing candidates for the fabrication of high-performance organic phase change materials (PCMs), but the stringent fabrication process and poor processability greatly hampered their commercialization. Herein, flexible leakage-proof composite PCMs with pronounced comprehensive performance are fabricated by a scalable polymer swelling strategy without using any solvent, in which the paraffin wax (PW) segment is confined in a robust flexible 3D polymer network, giving rise to the composite PCMs with excellent form stability even at 160 °C, a high latent heat energy storage density of 133.6 J/g, and an outstanding thermal conductivity of up to ∼5.11 W/mK. More importantly, the mass production of the flexible composite phase change fiber, film, and bulk products can be achieved by adopting mature processing technologies. These resultant composite PCMs exhibit promising thermal management ability to solve the overheating problem of electronics and high-efficiency solar-thermal energy conversion capacity.

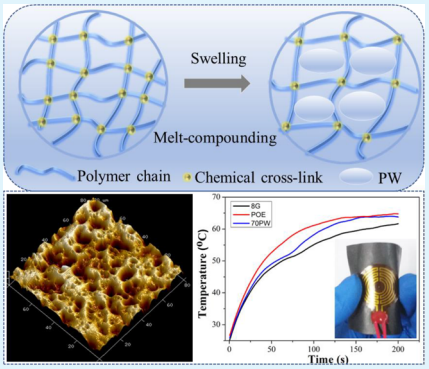

KEYWORDS: *flexible phase change materials, swollen polymer network structure, thermal conductivity, thermal management, energy conversion*

1. INTRODUCTION

Effective thermal management is of crucial significance to prevent the overheating problem of electronics such as integrated systems, batteries, laser instruments, radars, and flexible devices.[1−6] Recently, high-performance organic solid−liquid phase change materials (PCMs) capable of storing and releasing energy in the form of latent heat have attracted increasing attention.[7−9] In addition to thermal management, the utilization of solar energy associated with PCMs is a promising way to develop a green energy conversion supply chain. However, the application of organic PCMs in the thermal management of cutting-edge technologies has been significantly hampered by their low thermal conductivity (k, 0.2−0.4 W/mK) and liquid leakage, restricting energy charging/discharging rates and threatening the safety of devices and energy conversion systems.[10−15]

Considerable efforts have been made in incorporating 3D porous structural materials including graphene aerogels,[16−18] carbon foams,[19−21] carbon nanotube (CNT) sponge,[22] melamine foam (MF),[23,24] cellulose-based aerogels,[25] and metallic foams[26,27] into a phase change working ingredient to fabricate shape-stabilized PCMs.[28] It has been demonstrated that constructing 3D porous structural materials with a microcellular structure contributes to simultaneously overcoming the aforementioned shortcomings.[29−31] For example, Li et al.[19] prepared carbon aerogels by biomass carbonization employing melons as raw materials, followed by the vacuum infiltration of melted paraffin wax (PW). The maximum PW loading in the composite PCMs can reach up to 95 wt % with a latent heat of 126.9 J/g. Zhou et al.[32] fabricated graphene aerogels through directional freezing of polygamic acid salt/graphene oxide suspension, followed by freeze-drying, imidization, and graphitization. After impregnation of PW, the resultant PCMs show a high k (8.87 W/mK in the longitudinal direction) and the maximum PW loading in composite PCMs can reach up to 98.7 wt %. However, the size of these rigid 3D structural materials is limited by stringent fabrication methods (hydrothermal processes,[33,34] freeze-drying technology,[35] ice-templating self-assembly,[25,36] vacuum filtration,[37] chemical vapor deposition (CVD),[34] and biomass carbonization[19,38]) and the corresponding high cost.[39,40] It is highly expected to develop cost-effective fabrication routes to achieve mass production and narrow the mismatch between experimental preparation and industrial production.[39,41]

To impart flexibility to organic PCMs, it is a wise solution to use polymer supporting materials with a relatively high melting temperature as a substitute for inorganic 3D porous scaffolds.[42]

Received: October 18, 2021
Accepted: November 24, 2021
Published: December 2, 2021

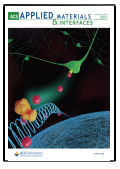

Downloaded from pubs.acs.org/aamick/article-pdf/13/49/59364/1279884/am1c20147.pdf by DOKUZ EYLUL UNIV user on 05 September 2026

© 2021 American Chemical Society

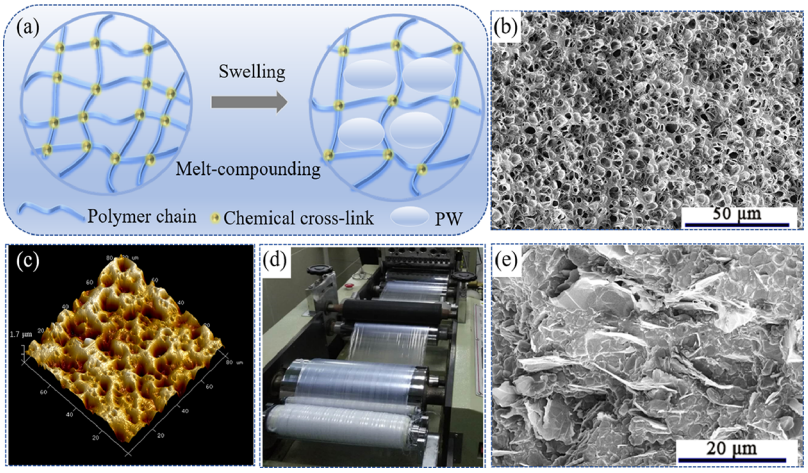

Figure 1. (a) Schematic representation of the polymer swelling strategy to fabricate flexible PW/POE composite PCMs. (b) Scanning electron microscopy (SEM) and (c) atomic force microscopy (AFM) images of 70PW composites in which PW was etched with methylene chloride. (d) Scalable manufacturing of flexible PW/POE films with the PW content of 50 wt % using the facile tape casting technology and (e) SEM images of 8G composites.

PW/high density polyethylene(HDPE),[43] PW/polypropylene,[44] hexadecane/ethylene-α-octene block copolymer (OBC),[45] PW/epoxy resin,[46] PW/polyamide/OBC,[47] and PW/styrene−butadiene−styrene triblock copolymer (SBS)[48] have been fabricated via melt-compounding approaches, in which the thermoplastic resins serve as supporting components to prevent the leakage of organic PCMs.[49,50] Previous studies have demonstrated that confining a phase change working ingredient in the polymer matrix instead of inorganic 3D porous structural materials is an effective shape-stabilization approach to fabricate flexible PCMs, but the poor form stability under higher temperature and low latent heat of those PCMs is still a challenge.[51,52]

Furthermore, owing to the fact that the active terminal hydroxyl groups of polyethylene glycol (PEG) are able to react with a crosslinker such as isocyanate and diisocyanate biuret, flexible polyurethane (PU)-based PCMs have been extensively studied using chemical approaches recently.[32,53−58] Specifically, the fabrication process includes crosslinking copolymerization of PEG with a crosslinker, chain extending, and chemical grafting.[32] Chen et al.[58] fabricated poly(glycidyl methacrylate)/carboxyl PEG PCMs through the ring-opening crosslinking reaction of carboxyl groups and epoxy groups, and the latent heat storage capacity of PCMs could reach to 70 J/g. Zhu et al.[59] synthesized poly(hydroxybutyrate-*co*-hydroxyvalerate)/PEG PCMs by free-radical solution polymerization, obtaining high temperature-resistant PCMs with a latent heat storage capacity of 107 J/g. However, most of those flexible polymeric PCMs were usually fabricated by complicated and environmentally unfriendly methods involving solvent and exhibited a low k (Table S1, Supporting Information).[60,61] Therefore, it is urgent to develop a facile, versatile, low-cost, and environmentally friendly route to fabricate flexible PCMs with excellent shape stability, high latent heat, and enhanced k.

Herein, flexible shape-stabilized PCMs with excellent overall performance were fabricated by a novel scalable polymer swelling strategy using PW as a phase change working ingredient and crosslinked polyolefin elastomer (POE) as a robust polymeric supporting material, in which PW segments were effectively confined within robust crosslinked polymer 3D network structures. Meanwhile, highly thermally conductive graphene nanoplatelets (GNPs) were employed as a thermally conductive filler to ameliorate the thermal charging/discharging rates of PCMs. The resultant flexible PCMs exhibited a stable latent heat of 133.6 J/g, a high in-plane k of up to ∼5.11 W/mK, and pronounced shape stability even with a temperature resistance of 160 °C. Thus, a promising and versatile route to massively produce flexible shape-stabilized PCMs is provided for the thermal management of electronics and solar-thermal energy conversion.

2. EXPERIMENTAL SECTION

2.1. Raw Materials. Polyolefin elastomer (POE, 8180, Dow Chemical Co., Ltd., America), graphene nanoplatelets (GNPs, GT-G03, Xiamen Knano Graphene Technology, Co., Ltd., China) with an average particle size of 10−20 μm, dicumyl peroxide (DCP, Nanjing Chemical Reagent Co., Ltd.), and paraffin wax (PW, Shanghai Hualing Recovery Equipment Factory, China) with the melting point of 53 °C were used.

2.2. Preparation of PW/POE/GNPs Composite PCMs. All the composites were fabricated by a scalable melt-compounding method based on a polymer swelling strategy (Figure S1, Supporting Information). First, POE was crosslinked by DCP (0.7 phr) at 150 °C for 5 min in an internal mixer (XSS-300, Shanghai Kechuang Rubber Plastics Machinery Set Ltd., China). The weight swelling ratio of pure POE and crosslinked POE with different contents of DCP was systematically studied (Figure S2, Supporting Information). Then, a certain amount of PW and crosslinked POE was mixed in the internal mixer at 150 °C for 10 min to obtain PW/POE composites, followed by the addition of GNPs and then mixing for another 5 min to obtain PW/POE/GNPs composite PCMs. The maximum content of PW can reach up to 70 wt % in PW/POE composites, and the mass ratio of PW to crosslinked POE was selected and fixed to be 70:30 in the PW/POE/GNPs composite. The loadings of GNPs in the PW/POE/GNPs composite were 4, 6, and 8 wt %, respectively. Also, noncrosslinked POE was used to fabricate the PW/POE/GNPs composite PCMs as a control. We found that the crosslinked POE with a more robust network structure was able to confine more PW than noncrosslinked POE (Figure S3, Supporting Information). Last, the resultant composite PCMs were hot-compressed into 10 cm × 10 cm × 200 μm films at 150 °C and 10 MPa for 5 min. The composites were designated according to the composition and filler loading. For example, "70PW" means the composites with 70 wt % PW and 30 wt % crosslinked POE, and "8G" means the composites with 8 wt % GNPs and 92 wt % PW/POE composites.

Downloaded from pubs.acs.org/aamick/article-pdf/13/49/59364/1279884/aam1c20147.pdf by DOKUZ EYLUL UNIV user on 05 September 2026

https://doi.org/10.1021/acsami.1c20147
ACS Appl. Mater. Interfaces 2021, 13, 59364−59372

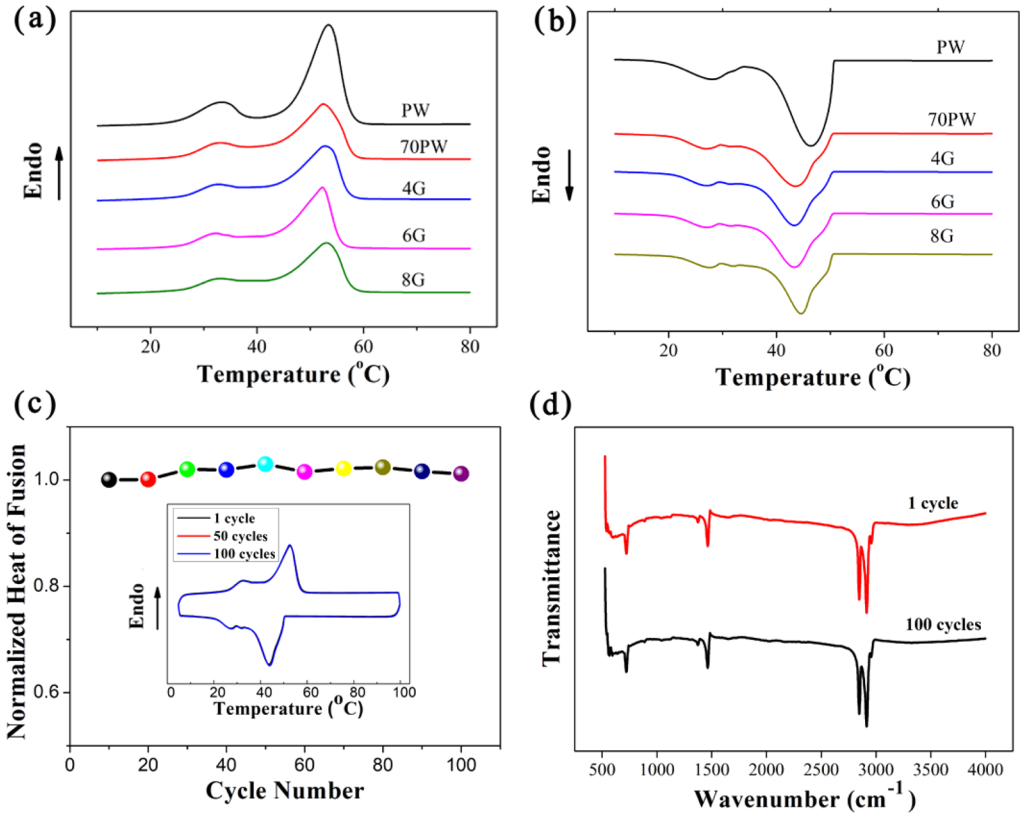

Figure 2. DSC (a) heating and (b) cooling scans of pure PW and PW/POE/GNPs composite PCMs. (c) Mass specific heat of fusion normalized by the first heating cycle (the inset shows the DSC curves of 8G composite PCMs within 100 thermal cycles). (d) FTIR spectra of 8G composite PCMs before and after 100 thermal cycles. The composites were designated according to the composition and filler loading.

In addition, the widely used scalable tape casting technology was also tried to fabricate the flexible PW/POE composite PCM films with the thickness of 30−60 μm, and the maximum content of PW can reach up to 50 wt % in PW/POE composites. The morphologies of PCM films fabricated by the tape casting technology can be found in Figure S4, Supporting Information.

2.3. Characterization. The morphologies of the composite PCMs were determined by scanning electron microscopy (SEM, JEOL JSM-5900LV, Japan) and atomic force microscopy (AFM, Multimode 8, Bruker, USA). The thermophysical properties of the composite PCMs were characterized by differential scanning calorimetry (DSC, Q20, TA Instruments, USA) at a scanning rate of 10 °C min^{-1} under a purified nitrogen atmosphere. The k of the composite PCMs was measured by the laser flash technique (Netzsch, LFA 467, USA) and calculated from $k = \alpha \times \rho \times C_p$, where α, ρ, and C_p represent the thermal diffusivity (m^2/s), density (g/cm^3), and specific heat capacity (J/(g·K)) of the samples, respectively. The detailed information concerning the thermal conductivity of composite PCMs can be found in Table S2, Supporting Information. The temperature dependence of the storage modulus (G') of the samples was measured by a stress-controlled rheometer (AR2000, TA Instruments, USA) equipped with parallel-plate geometry. The optical properties of the 8G sample were characterized using an ultraviolet−visible−near-infrared spectrophotometer (UV−vis−NIR, UV3600, Shimadzu, Japan) in the wavelength range of 200−1800 nm. X-ray diffraction (XRD) patterns of the composite PCMs were measured by a Rigaku Ultima IV diffractometer (Rigaku, Japan) with Cu Kα radiation (λ = 0.15406 nm) at a voltage of 40 kV and a current of 40 mA. The mechanical properties of the composite PCMs were tested by a universal material testing machine (Instron 5967, USA).

3. RESULTS AND DISCUSSION

As shown in Figure 1a, the flexible PW/POE/GNPs composite PCMs were fabricated by a facile polymer swelling strategy using PW as the phase change working ingredient and crosslinked POE as the robust polymeric supporting material. Owing to the excellent chemistry compatibility between PW and POE, the crosslinked polymer network can be swollen by the molten small-molecule PW during the melt-compounding process. Briefly, dicumyl peroxide (DCP) was used as the curing agent to crosslink POE linear chains, accompanied by strong overlapping with each other. The formed chemically crosslinked network only contains relatively stable carbon−carbon bonds as junction units, which endow the 3D polymer network with excellent thermal stability and superior heat-aging resistance. Then, PW with a melting point of 53 °C was added and mixed with the crosslinked POE at 150 °C. Although crosslinked POE is unable to melt because of the chemically crosslinked network, an enormous amount of molten PW with a small molecule can be soaked and confined in the crosslinked polymer network.

For polymer dissolution, the swelling process is the first step in the interaction between the polymer network and solvent molecules, followed by solvation of polymer molecules. However, the chemically crosslinking bonds in polymers can effectively prevent the dissolution of polymers in solvent.[62] Thus, the crosslinked POE with a more robust network structure was able to confine more PW than noncrosslinked POE (Figure S2, Supporting Information). The swelling process of polymer materials can be described by the Flory−Rehner theory, which compares the entropic contribution of the polymer and solvent with the elastic energy created by the swollen polymer network (eq 1).[63]

https://doi.org/10.1021/acsami.1c20147
ACS Appl. Mater. Interfaces 2021, 13, 59364−59372

Downloaded from pubs.acs.org/aamick/article-pdf/13/49/59364/1279884/am1c20147.pdf by DOKUZ EYLUL UNIV user on 05 September 2026

$$\frac{1}{M_c} = \frac{2}{M_n} - \frac{\ln(1-\varphi_s) + \varphi_s + \chi\varphi_s^2}{V_1\rho_d\left[\varphi_s^{1/3} - \frac{\varphi_s}{2}\right]} \quad (1)$$

where M_c, M_n, φ_s, χ, V_1, and ρ_d are the average molecular weight between crosslinks, the average molecular weight of the polymer chains prior to crosslinking, the volume fraction of the polymer at the swelling equilibrium state, the polymer−solvent interaction parameter, the molar volume of the solvent, and the dry density of the polymer network, respectively.[63] The model suggests excellent chemistry compatibility between the polymer and solvent, and an appropriate crosslinked degree is desired to obtain a high swelling degree. The weight swelling ratio of pure POE and crosslinked POE by different contents of DCP was systematically studied, and we found that 0.7 phr DCP is more desired to obtain the highest weight swelling ratio (Figure S2, Supporting Information).

From Figure 1b,c, the crosslinked polymer swelling process isolated PW phase domains with the size of about 2 μm uniformly dispersed in the continuous crosslinked POE phase. The molecular chains of the PW phase are effectively confined in the robust crosslinked network structure to significantly prevent the leakage of liquid PW, giving rise to the improvement of the form stability of PCMs. Different from the widely used crosslinking copolymerization methods to synthesize PU-based PCMs, scalable melt-compounding techniques such as melt-mixing and tape casting can be used to fabricate the high-performance PCMs based on the polymer swelling strategy. Figure 1d shows the large-scale flexible PW/POE films with the thickness of 30−60 μm using a facile tape casting technology. Furthermore, GNPs as thermally conductive components were added into the POE/PW composites to enhance the k and light-to-heat conversion ability of PCMs. Meanwhile, two-dimensional (2D) GNP sheets with a large aspect ratio are oriented along the in-plane direction, which is beneficial to the extraordinary in-plane k of composite phase change films (Figure 1e).

The thermal properties including phase change temperature, latent heat capacities, and thermal reproducibility were tested by DSC analysis. There are two well-defined separated peaks corresponding to the homogeneously nucleated crystal−rotator transition and heterogeneously nucleated rotator−liquid transition of PW that existed both in the melting and cooling processes (Figure 2a,b).[64] The detailed melting and crystallization parameters including melting/crystallization enthalpy ($\Delta H_m/\Delta H_c$) and melting/crystallization peak temperature (T_{mp}/T_{cp}) are summarized in Table 1. The results demonstrated that both the T_{cp} and T_{mp} of the composite PCMs shift to a lower temperature after PW is encapsulated in crosslinked POE in the composites, which can be attributed to the confinement of the PW chains in the crosslinked 3D network structure and restriction of their movement during phase transition.[35] After introducing GNPs, a negligible change in phase change temperature is observed. The phase change enthalpies of composite PCMs decrease with the introduction of the crosslinked POE supporting network and GNPs because a portion of working substance is replaced by substances without energy storage capacity. Nonetheless, the high-performance composite PCMs with the GNP loading of 8 wt % exhibit a decent latent heat energy storage density of up to 130.2 J g^{-1}, which meets the general requirements of thermal management and energy conversion applications. To validate the thermal stability of composite PCMs, the 8G sample was heated and cooled in the range of 5−100 °C for 100 cycles, as shown in Figure 2c. There are no obvious changes in phase change behaviors from DSC curves and the position of characteristic peaks from the FTIR spectra after 100 thermal cycles, demonstrating that the obtained composite PCMs presented excellent thermal stability (Figure 2d). Also, the thermogravimetric characterization also has been conducted to further confirm the thermal stability of composite PCMs (Figure S5).

Table 1. DSC Heating and Cooling Characteristics of Pure PW and PW/POE/GNPs Composite PCMs.

sample	T_{cp} (°C)	ΔH_c (J g^{-1})	T_{mp} (°C)	ΔH_m (J g^{-1})
PW	46.4	198.4	53.4	201.1
70PW	43.5	146.8	52.4	149.1
4G	43.4	136.6	52.7	141.1
6G	44.6	133.6	52.3	134.4
8G	43.1	130.2	53.0	133.6

The shape-stability test of flexible PCMs was conducted by a leakage test and recorded by using digital camera observation, as shown in Figure 3a. When heated to 160 °C, 70PW and 8G composite PCMs maintain the original shape without any liquid leakage, indicating that the robust crosslinked POE polymer network can effectively improve the form stability of the organic PCMs. On the contrary, obvious liquid leakage is observed for pure PW when heated to 60 °C, a little above its melting temperature. It is worth noting that when the crosslinked POE is swollen by small-molecule PW in the melt-compounding process, its plasticity recovers due to the plasticizing effect of PW molecules, and the obtained shape-stabilized PCMs exhibited outstanding flexibility and processability, which can be processed into various shapes such as fiber, film, and bulk through facile and conventional melt-compounding techniques (Figure S6, Supporting Information). A superfoldable 8G film with the size of 10 cm × 10 cm × 200 μm can be folded into a crane without liquid leakage at 80 °C (Figure 3a, right).

To better understand the shape stability of the flexible PCMs, dynamic rheological tests were used to detect the storage modulus of pure PW and composite PCMs. Figure 3b depicts the temperature dependence of the storage modulus (G') of pure PW, 70PW, and 8G over the range from 40 to 200 °C. For pure PW, the G' of pure PW displays a dramatic decrease and becomes undetectable soon once the temperature is higher than 50 °C, indicating that pure PW has melted and liquid leakage has taken place. However, for the 70PW sample, a decrease in G' also exists around 60 °C owing to the softening of the sample, but the G' remains detectable in the range of 60−200 °C, indicating that the molten PW is still confined in the robust 3D crosslinked polymer network and maintains excellent shape stability. In comparison to 70PW, the G' of 8G remains at an even higher level. This is because the GNPs form a filler network in the matrix, which further suppresses the long-range motion of the PW segment. The rheological results are in good accordance with the digital camera observation (Figure 3a). The above results suggest that the robust crosslinked POE network can accommodate the molten PW well and endow the composite PCMs with excellent shape stability owing to the crosslinked polymer network and filler network.

The k of POE/PW/GNPs composite PCMs with various filler loadings is presented in Figure 3c. Both the through-plane

Downloaded from pubs.acs.org/aamick/article-pdf/13/49/59364/1279884/am1c20147.pdf by DOKUZ EYLUL UNIV user on 05 September 2026

https://doi.org/10.1021/acsami.1c20147
ACS Appl. Mater. Interfaces 2021, 13, 59364−59372

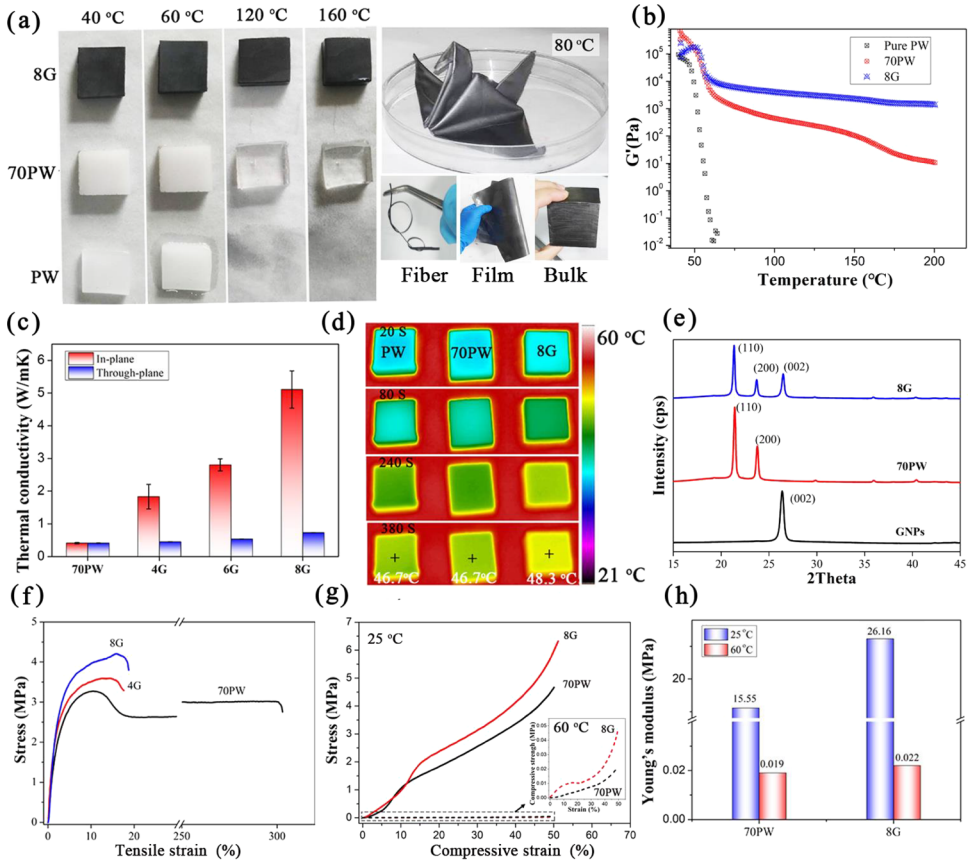

Figure 3. (a) Shape-stability test of pure PW, 70PW, and 8G with increasing temperature. (b) Temperature dependence of the storage modulus (G') of pure PW, 70PW, and 8G from 40 to 200 °C. (c) Through-plane and in-plane k of the composite with different GNP loadings. (d) Thermal response behaviors of pure PW, 70PW, and 8G samples. (e) XRD patterns of pure PW, 70PW, and 8G samples. (f) Typical tensile stress−strain curves of 70PW, 4G, and 8G at 25 °C. (g) Typical compressive stress−strain curves of 70PW and 8G at 25 and 60 °C. (h) Young's modulus of 70PW and 8G at 25 and 60 °C obtained from the compressive test.

and in-plane k increase greatly with the increase in GNP loading. The through-plane and in-plane k of POE/PW/GNPs composite PCMs with a GNP loading of 8 wt % can reach to 0.73 and 5.1 W/mK, respectively, and the corresponding k enhancements are 823 and 900% compared with 70PW with a k of 0.41 W/mK. Note that the prominent anisotropic k is well consistent with the anisotropic laminated structure, and two-dimensional fillers with a large aspect ratio can easily achieve good alignment along the flow direction in compression processing (Figure 1e). In addition, the thermal response behavior of pure PW, 70PW, and 8G was recorded by using an infrared thermal imager. The temperature increase of 8G is faster than those of PW and 70PW owing to the fact that a higher through-plane k enables the composite PCMs to transfer thermal energy more rapidly (Figure 3c, right). Consequently, the thermal charging/discharging rates of composite PCMs are greatly enhanced by oriented GNPs, while there is no significant effect on the crystallization behaviors of PW as confirmed by XRD patterns (Figure 3d). In comparison with previously reported flexible PCMs fabricated by crosslinking copolymerization or the melt blending method (Table S1, Supporting Information),[32,53−58] the fabricated PCMs in this work have a relatively high k and superior energy storage ability.

In addition to shape stability and k, the mechanical performance of flexible composite PCMs was investigated *via* tensile and compression tests. The typical tensile stress−strain curves of 70PW, 4G, and 8G are shown in Figure 3e. The POE/PW PCMs possess excellent mechanical property with the elongation at break of up to 300%, which is a significant achievement for highly crystalline organic PCMs. After adding inorganic fillers, the elongation at break of thermally conductive composite PCMs filled with a large number of GNPs is greatly depressed owing to the unavoidable stress concentrations and weak interactions between the fillers and matrices. Nevertheless, the tensile strength and elongation at break of 8G are still maintained at a relatively high level, reaching ∼4.2 MPa and ∼18.75%, respectively. Interestingly, when PW in the composites melts at 60 °C, the flexible PCMs can be also compressed due to the existing POE polymer network structure (Figure 3f), and Young's modulus of 8G at 60 °C significantly decreases to 0.022 MPa (Figure 3g). Notably, the thermally conductive composite PCMs with such high conformability are helpful to reduce the thermal contact resistance when used as thermal interface materials (TIMs), exhibiting great potentials in the thermal management of electronics.[65]

To evaluate the practical thermal transfer and storage performance of the flexible composite PCMs, the thermal management of electronics and solar-thermal energy conversion and storage tests were carried out based on the high-performance composites. As shown in Figure 4a, the flexible PCMs can be used as the thermal management materials of electronic chips and flexible electronics to relieve their

Downloaded from pubs.acs.org/aamick/article-pdf/13/49/59364/12798844/am1c20147.pdf by DOKUZ EYLUL UNIV user on 05 September 2026

https://doi.org/10.1021/acsami.1c20147
ACS Appl. Mater. Interfaces 2021, 13, 59364−59372

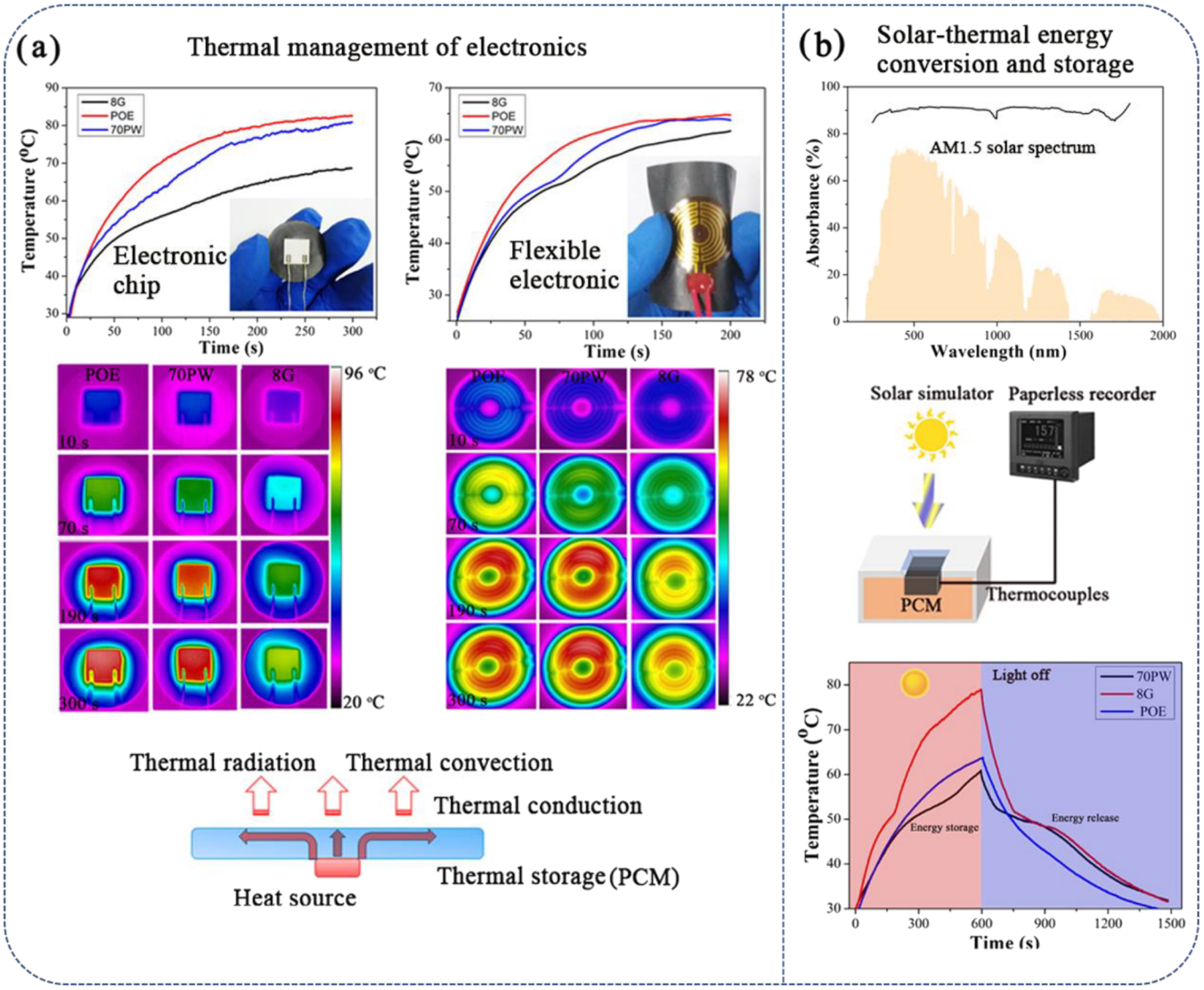

Figure 4. Applications of flexible composite PCMs for (a) thermal management of electronics and (b) solar-thermal energy conversion and storage.

overheating problem. The surface temperature variation of electronic devices was recorded by thermocouples and a thermal infrared camera. As a result, the temperature of electronic devices rises slowly and exhibits a lower equilibrium temperature when 8G and 70PW composites are used as thermal management materials compared with pure POE. An obvious platform successfully emerges in the range of 50−60 °C, indicating that a solid−liquid phase change has taken place for the composite PCMs and a large amount of heat is effectively stored in the form of latent heat instead of sensible heat. A closer inspection indicates that the heat dissipation efficiency of 8G is more significant than that of 70PW owing to the higher *k*. Thus, the phase change films with a high in-plane *k* can effectively spread the thermal energy from localized hot spots of the heat source to a larger area, further making more efficient use of the thermal convection, thermal radiation, and thermal storage to significantly reduce the temperature of electronics and allowing electronics to safely work for an extended period of time without exceeding the upper temperature limits. An elegant coupling of the phase change energy storage and high *k* plays a pivotal role in the thermal management applications, offering guidance to solve the heat dissipation of advanced electronic devices.

On the other hand, a light-to-thermal energy conversion system was designed to evaluate the practical thermal energy storage performance, and the light-to-heat conversion curves under 1 sun intensity (1 kW/m^2) are presented in Figure 4b. In our previous work,[66] the addition of GNPs can not only improve the *k* but also enhance the photoabsorption performance of PCMs. As expected, the 8G composites exhibit high absorbance (>85%) over a wide wavelength region, which is beneficial to the harvesting of solar energy. Also, the solar-thermal conversion efficiency (STCE) of the PCM system has been calculated according to the photo-thermal calculation equation,[34] and the STCE of the 8G sample can reach to 78%. When light is turned on, the 8G composite shows a more significant temperature increase than pure POE and 70PW samples due to the improved heat transfer and photo-absorption capacities (Figure 4b). Compared with 70PW, the time to complete phase transition for 8G is greatly shortened after removing the illumination, and 8G and 70PW composites show another obvious temperature platform in the range of 50−60 °C, indicating that the stored phase change latent heat

https://doi.org/10.1021/acsami.1c20147
ACS Appl. Mater. Interfaces 2021, 13, 59364−59372

Downloaded from pubs.acs.org/aamick/article-pdf/13/49/59364/1798844/am1c20147.pdf by DOKUZ EYLUL UNIV user on 05 September 2026

at the irradiation period is released to maintain the temperature of the composite PCMs. By contrast, there are no melting and cooling plateaus in the whole process for pure POE. It is thus clear that the flexible PCMs present a promising thermal storage performance for energy-related applications.

4. CONCLUSIONS

In summary, high-performance flexible composite PCMs were achieved by a novel polymer swelling strategy using PW as the phase change working ingredient and crosslinked POE as the robust polymeric supporting skeleton. The fabricated PW/POE/GNPs composite PCMs exhibit enhanced comprehensive performance, including excellent shape stability at 160 °C, a considerable energy storage density (133.6 J/g), and an outstanding in-plane k of up to ~5.11 W/mK. More importantly, owing to their outstanding processability, the composite PCMs obtained from the polymer swelling strategy can be processed into various products such as fiber, film, and bulk through scalable melt-compounding techniques such as compression molding and tape casting, providing an easy-to-implement strategy to achieve scalable manufacture of flexible PCMs without any solvent. Finally, the practical thermal transfer and storage performance of the thermally conductive leakage-roof flexible composite PCMs were confirmed by demonstrative field tests, showing great application potentials in the thermal management of electronics and solar energy conversion.

■ ASSOCIATED CONTENT

Supporting Information

The Supporting Information is available free of charge at https://pubs.acs.org/doi/10.1021/acsami.1c20147.

Summary of properties of flexible polymeric PCMs; schematic representation of the crosslinked polymer network swelling strategy; weight swelling ratio of pure POE and crosslinked POE; optical images of pure POE and crosslinked POE after PW swelling; detailed information concerning thermal conductivity; optical images of the PW/POE composite in an internal mixer; SEM images of the PW/POE composite with 50 wt % PW; TGA curves of the PW/POE composite; photographs of PW/POE/GNPs composite PCMs with various shapes (PDF)

■ AUTHOR INFORMATION

Corresponding Authors

Chang-Ping Feng − *College of Polymer Science and Engineering, State Key Laboratory of Polymer Materials Engineering, Sichuan University, Chengdu 610065 Sichuan, People's Republic of China; Shandong Engineering Research Center for Additive Manufacturing, Qingdao University of Technology, Qingdao 266520 Shandong, People's Republic of China;* orcid.org/0000-0003-3070-9021; Phone: +86 28 8546 0130; Email: fengc_p@163.com

Wei Yang − *College of Polymer Science and Engineering, State Key Laboratory of Polymer Materials Engineering, Sichuan University, Chengdu 610065 Sichuan, People's Republic of China;* orcid.org/0000-0003-0198-1632; Email: weiyang@scu.edu.cn

Authors

Fang Wei − *College of Polymer Science and Engineering, State Key Laboratory of Polymer Materials Engineering, Sichuan University, Chengdu 610065 Sichuan, People's Republic of China*

Jie Yang − *College of Polymer Science and Engineering, State Key Laboratory of Polymer Materials Engineering, Sichuan University, Chengdu 610065 Sichuan, People's Republic of China*

Lu-Yao Yang − *College of Polymer Science and Engineering, State Key Laboratory of Polymer Materials Engineering, Sichuan University, Chengdu 610065 Sichuan, People's Republic of China*

Lu Bai − *College of Polymer Science and Engineering, State Key Laboratory of Polymer Materials Engineering, Sichuan University, Chengdu 610065 Sichuan, People's Republic of China*

Rui-Ying Bao − *College of Polymer Science and Engineering, State Key Laboratory of Polymer Materials Engineering, Sichuan University, Chengdu 610065 Sichuan, People's Republic of China*

Zheng-Ying Liu − *College of Polymer Science and Engineering, State Key Laboratory of Polymer Materials Engineering, Sichuan University, Chengdu 610065 Sichuan, People's Republic of China*

Ming-Bo Yang − *College of Polymer Science and Engineering, State Key Laboratory of Polymer Materials Engineering, Sichuan University, Chengdu 610065 Sichuan, People's Republic of China;* orcid.org/0000-0001-7950-7645

Complete contact information is available at: https://pubs.acs.org/10.1021/acsami.1c20147

Notes

The authors declare no competing financial interest.

■ ACKNOWLEDGMENTS

This work was funded by the National Natural Science Foundation of China (NNSFC grant nos. 52103034, 51873126, and 52003170) and Shandong Provincial Natural Science Foundation (ZR2021QE014).

■ REFERENCES

(1) Huang, Y. H.; Cheng, W. L.; Zhao, R. Thermal Management of Li-ion Battery Pack with the Application of Flexible form-Stable Composite Phase Phange Materials. *Energy Convers. Manage.* **2019**, *182*, 9−20.

(2) Zhou, L.; Tao, X. F.; Tang, L. S.; Yang, M. B.; Yang, W. Waterproof Phase Change Material With Facilely Incorporated Cellulose Nanocrystal/Polyisopropyl Acrylamide Network for All-Weather Outdoor Thermal Energy Storage. *ACS Appl. Mater. Interfaces* **2020**, *12*, 53365−53375.

(3) Zhang, Y.; Chou, J. B.; Li, J.; Li, H.; Du, Q.; Yadav, A.; Zhou, S.; Shalaginov, M. Y.; Fang, Z.; Zhong, H.; Roberts, C.; Robinson, P.; Bohlin, B.; Rios, C.; Lin, H.; Kang, M.; Gu, T.; Warner, J.; Liberman, V.; Richardson, K.; Hu, J. Broadband Transparent Optical Phase Change Materials for High-Performance Nonvolatile Photonics. *Nat. Commun.* **2019**, *10*, 4279.

(4) Huang, X.; Chen, X.; Li, A.; Atinafu, D.; Gao, H.; Dong, W.; Wang, G. Shape-Stabilized Phase Change Materials Based on Porous Supports for Thermal Energy Storage Applications. *Chem. Eng. J.* **2019**, *356*, 641−661.

(5) Zou, D.; Ma, X.; Liu, X.; Zheng, P.; Hu, Y. Thermal Performance Enhancement of Composite Phase Change Materials (PCM) Using Graphene and Carbon Nanotubes as Additives for The Potential

Downloaded from pubs.acs.org/aamick/article-pdf/13/49/59364/12798844/am1c20147.pdf by DOKUZ EYLUL UNIV user on 05 September 2026

Application in Lithium-Ion Power Battery. *Int. J. Heat Mass Transfer* **2018**, *120*, 33−41.
(6) Feng, C. P.; Yang, L. Y.; Yang, J.; Bai, L.; Bao, R. Y.; Liu, Z. Y.; Yang, M. B.; Lan, H. B.; Yang, W. Recent Advances in Polymer-Based Thermal Interface Materials for Thermal Management: A Mini-Review. *Composites Communications* **2020**, *22*, 100528.
(7) Zalden, P.; Quirin, F.; Schumacher, M.; Siegel, J.; Wei, S.; Koc, A.; Nicoul, M.; Trigo, M.; Andreasson, P.; Enquist, H.; Shu, M. J.; Pardini, T.; Chollet, M.; Zhu, D.; Lemke, H.; Ronneberger, I.; Larsson, J.; Lindenberg, A. M.; Fischer, H. E.; Hau-Riege, S.; Reis, D. A.; Mazzarello, R.; Wuttig, M.; Sokolowski-Tinten, K. Femtosecond X-Ray Diffraction Reveals a Liquid−Liquid Phase Transition in Phase-Change Materials. *Science* **2019**, *364*, 1062−1067.
(8) Liu, H.; Tang, J.; Dong, L.; Wang, H.; Xu, T.; Gao, W.; Zhai, F.; Feng, Y.; Feng, W. Optically Triggered Synchronous Heat Release Of Phase-Change Enthalpy and Photo-Thermal Energy in Phase-Change Materials at Low Temperatures. *Adv. Funct. Mater.* **2021**, *31*, 2008496.
(9) Wang, J.; Yang, M.; Lu, Y.; Jin, Z.; Tan, L.; Gao, H.; Fan, S.; Dong, W.; Wang, G. Surface Functionalization Engineering Driven Crystallization Behavior of Polyethylene Glycol Confined in Mesoporous Silica for Shape-Stabilized Phase Change Materials. *Nano Energy* **2016**, *19*, 78−87.
(10) Zhang, Y.; Wang, J.; Qiu, J.; Jin, X.; Umair, M. M.; Lu, R.; Zhang, S.; Tang, B. Ag-Graphene/PEG Composite Phase Change Materials for Enhancing Solar-Thermal Energy Conversion and Storage Capacity. *Applied Energy* **2019**, *237*, 83−90.
(11) Zeng, J. L.; Chen, Y. H.; Shu, L.; Yu, L. P.; Zhu, L.; Song, L. B.; Cao, Z.; Sun, L. X. Preparation and Thermal Properties of Exfoliated Graphite/Erythritol/Mannitol Eutectic Composite as Form-Stable Phase Change Material for Thermal Energy Storage. *Sol. Energy Mater. Sol. Cells* **2018**, *178*, 84−90.
(12) Nazir, H.; Batool, M.; Bolivar Osorio, F. J.; Isaza-Ruiz, M.; Xu, X.; Vignarooban, K.; Phelan, P.; Inamuddin; Kannan, A. M. Recent Developments in Phase Change Materials for Energy Storage Applications: a Review. *Int. J. Heat Mass Transfer* **2019**, *129*, 491−523.
(13) Feng, C. P.; Chen, L. B.; Tian, G. L.; Bai, L.; Bao, R. Y.; Liu, Z. Y.; Ke, K.; Yang, M. B.; Yang, W. Robust Polymer-Based Paper-Like Thermal Interface Materials with a Through-Plane Thermal Conductivity Over 9 $Wm^{-1}K^{-1}$. *Chem. Eng. J.* **2020**, *392*, 123784.
(14) Deng, Y.; Li, J.; Qian, T.; Guan, W.; Li, Y.; Yin, X. Thermal Conductivity Enhancement of Polyethylene Glycol/Expanded Vermiculite Shape-Stabilized Composite Phase Change Materials with Silver Nanowire for Thermal Energy Storage. *Chem. Eng. J.* **2016**, *295*, 427−435.
(15) Tang, Z.; Gao, H.; Chen, X.; Zhang, Y.; Li, A.; Wang, G. Advanced Multifunctional Composite Phase Change Materials Based on Photo-Responsive Materials. *Nano Energy* **2021**, *80*, 105454.
(16) Chen, T.; Liu, C.; Mu, P.; Sun, H.; Zhu, Z.; Liang, W.; Li, A. Fatty Amines/Graphene Sponge Form-Stable Phase Change Material Composites with Exceptionally High Loading Rates and Energy Density for Thermal Energy Storage. *Chem. Eng. J.* **2020**, *382*, 122831.
(17) Wang, M.; Zhang, T.; Mao, D.; Yao, Y.; Zeng, X.; Ren, L.; Cai, Q.; Mateti, S.; Li, L. H.; Zeng, X.; Du, G.; Sun, R.; Chen, Y.; Xu, J. B.; Wong, C. P. Highly Compressive Boron Nitride Nanotube Aerogels Reinforced with Reduced Graphene Oxide. *ACS Nano* **2019**, *13*, 7402−7409.
(18) Liu, D.; Lei, C.; Wu, K.; Fu, Q. A Multidirectionally Thermoconductive Phase Change Material Enables High and Durable Electricity via Real-Environment Solar-Thermal-Electric Conversion. *ACS Nano* **2020**, *14*, 15738−15747.
(19) Li, Y.; Samad, Y. A.; Polychronopoulou, K.; Alhassan, S. M.; Liao, K. From Biomass to High Performance Solar−Thermal and Electric−Thermal Energy Conversion and Storage Materials. *J. Mater. Chem. A* **2014**, *2*, 7759−7765.
(20) Chen, X.; Gao, H.; Yang, M.; Dong, W.; Huang, X.; Li, A.; Dong, C.; Wang, G. Highly Graphitized 3D Network Carbon for Shape-Stabilized Composite Pcms with Superior Thermal Energy Harvesting. *Nano Energy* **2018**, *49*, 86−94.
(21) Kholmanov, I.; Kim, J.; Ou, E.; Ruoff, R. S.; Shi, L. Continuous Carbon Nanotube−Ultrathin Graphite Hybrid Foams for Increased Thermal Conductivity and Suppressed Subcooling in Composite Phase Change Materials. *ACS Nano* **2015**, *9*, 11699−11707.
(22) Aftab, W.; Mahmood, A.; Guo, W.; Yousaf, M.; Tabassum, H.; Huang, X.; Liang, Z.; Cao, A.; Zou, R. Polyurethane-Based Flexible and Conductive Phase Change Composites for Energy Conversion and Storage. *Energy Storage Materials* **2019**, *20*, 401−409.
(23) Wu, H. Y.; Chen, R. T.; Shao, Y. W.; Qi, X. D.; Yang, J. H.; Wang, Y. Novel Flexible Phase Change Materials with Mussel-Inspired Modification of Melamine Foam for Simultaneous Light-Actuated Shape Memory and Light-to-Thermal Energy Storage Capability. *ACS Sustainable Chem. Eng.* **2019**, *7*, 13532−13542.
(24) Wu, H. Y.; Li, S. T.; Shao, Y. W.; Jin, X. Z.; Qi, X. D.; Yang, J. H.; Zhou, Z. W.; Wang, Y. Melamine Foam/Reduced Graphene Oxide Supported Form-Stable Phase Change Materials with Simultaneous Shape Memory Property and Light-to-Thermal Energy Storage Capability. *Chem. Eng. J.* **2020**, *379*, 122373.
(25) Wei, X.; Xue, F.; Qi, X. D.; Yang, J. H.; Zhou, Z. W.; Yuan, Y. P.; Wang, Y. Photo-and Electro-Responsive Phase Change Materials Based on Highly Anisotropic Microcrystalline Cellulose/Graphene Nanoplatelet Structure. *Applied Energy* **2019**, *236*, 70−80.
(26) Wang, C.; Lin, T.; Li, N.; Zheng, H. Heat Transfer Enhancement of Phase Change Composite Material: Copper Foam/Paraffin. *Renewable Energy* **2016**, *96*, 960−965.
(27) Ghalambaz, M.; Zhang, J. Conjugate Solid-Liquid Phase Change Heat Transfer in Heatsink Filled with Phase Change Material-Metal Foam. *Int. J. Heat Mass Transfer* **2020**, *146*, 118832.
(28) Xie, N.; Luo, J.; Li, Z.; Huang, Z.; Gao, X.; Fang, Y.; Zhang, Z. Salt Hydrate/Expanded Vermiculite Composite as a Form-Stable Phase Change Material for Building Energy Storage. *Sol. Energy Mater. Sol. Cells* **2019**, *189*, 33−42.
(29) Chen, X.; Gao, H.; Hai, G.; Jia, D.; Xing, L.; Chen, S.; Cheng, P.; Han, M.; Dong, W.; Wang, G. Carbon Nanotube Bundles Assembled Flexible Hierarchical Framework Based Phase Change Material Composites for Thermal Energy Harvesting and Thermotherapy. *Energy Storage Materials* **2020**, *26*, 129−137.
(30) Jia, X.; Li, Q.; Ao, C.; Hu, R.; Xia, T.; Xue, Z.; Wang, Q.; Deng, X.; Zhang, W.; Lu, C. High Thermal Conductive Shape-Stabilized Phase Change Materials of Polyethylene Glycol/Boron Nitride@Chitosan Composites for Thermal Energy Storage. *Composites Part A: Applied Science and Manufacturing* **2020**, *129*, 105710.
(31) Yang, J.; Li, X.; Han, S.; Zhang, Y.; Min, P.; Koratkar, N.; Yu, Z.-Z. Air-Dried, High-Density Graphene Hybrid Aerogels for Phase Change Composites with Exceptional Thermal Conductivity and Shape Stability. *J. Mater. Chem. A* **2016**, *4*, 18067−18074.
(32) Zhou, Y.; Liu, X.; Sheng, D.; Lin, C.; Ji, F.; Dong, L.; Xu, S.; Wu, H.; Yang, Y. Polyurethane-Based Solid-Solid Phase Change Materials with in Situ Reduced Graphene Oxide for Light-Thermal Energy Conversion and Storage. *Chem. Eng. J.* **2018**, *338*, 117−125.
(33) Yang, J.; Tang, L.-S.; Bai, L.; Bao, R.-Y.; Liu, Z.; Xie, B.-H.; Yang, M.-B.; Yang, W. Photodriven Shape-Stabilized Phase Change Materials with Optimized Thermal Conductivity by Tailoring the Microstructure of Hierarchically Ordered Hybrid Porous Scaffolds. *ACS Sustainable Chem. Eng.* **2018**, *6*, 6761−6770.
(34) Yang, J.; Qi, G.-Q.; Bao, R.-Y.; Yi, K.; Li, M.; Peng, L.; Cai, Z.; Yang, M.-B.; Wei, D.; Yang, W. Hybridizing Graphene Aerogel into Three-Dimensional Graphene Foam for High-Performance Composite Phase Change Materials. *Energy Storage Materials* **2018**, *13*, 88−95.
(35) Yang, J.; Tang, L. S.; Bao, R. Y.; Bai, L.; Liu, Z. Y.; Xie, B. H.; Yang, M. B.; Yang, W. Hybrid Network Structure Of Boron Nitride and Graphene Oxide in Shape-Stabilized Composite Phase Change Materials with Enhanced Thermal Conductivity and Light-to-Electric Energy Conversion Capability. *Sol. Energy Mater. Sol. Cells* **2018**, *174*, 56−64.

Downloaded from pubs.acs.org/aamick/article-pdf/13/49/59364/1279884/am1c20147.pdf by DOKUZ EYLUL UNIV user on 05 September 2026

https://doi.org/10.1021/acsami.1c20147
ACS Appl. Mater. Interfaces 2021, 13, 59364−59372

(36) Ye, S.; Zhang, Q.; Hu, D.; Feng, J. Core−Shell-Like Structured Graphene Aerogel Encapsulating Paraffin: Shape-Stable Phase Change Material for Thermal Energy Storage. *J. Mater. Chem. A* **2015**, *3*, 4018−4025.
(37) Zhang, L.; Zhou, K.; Wei, Q.; Ma, L.; Ye, W.; Li, H.; Zhou, B.; Yu, Z.; Lin, C. T.; Luo, J.; Gan, X. Thermal Conductivity Enhancement of Phase Change Materials with 3D Porous Diamond Foam for Thermal Energy Storage. *Applied Energy* **2019**, *233-234*, 208−219.
(38) Wei, Y.; Li, J.; Sun, F.; Wu, J.; Zhao, L. Leakage-Proof Phase Change Composites Supported by Biomass Carbon Aerogels from Succulents. *Green Chem.* **2018**, *20*, 1858−1865.
(39) Yang, J.; Zhang, E.; Li, X.; Zhang, Y.; Qu, J.; Yu, Z. Z. Cellulose/Graphene Aerogel Supported Phase Change Composites with High Thermal Conductivity and Good Shape Stability for Thermal Energy Storage. *Carbon* **2016**, *98*, 50−57.
(40) Wang, B.; Li, G.; Xu, L.; Liao, J.; Zhang, X. Nanoporous Boron Nitride Aerogel Film and its Smart Composite with Phase Change Materials. *ACS Nano* **2020**, 16590.
(41) Zhou, L.; Tang, L. S.; Tao, X. F.; Yang, J.; Yang, M. B.; Yang, W. Facile Fabrication of Shape-Stabilized Polyethylene Glycol/Cellulose Nanocrystal Phase Change Materials Based on Thiol-Ene Click Chemistry and Solvent Exchange. *Chem. Eng. J.* **2020**, *396*, 125206.
(42) Umair, M. M.; Zhang, Y.; Iqbal, K.; Zhang, S.; Tang, B. Novel Strategies and Supporting Materials Applied to Shape-Stabilize Organic Phase Change Materials for Thermal Energy Storage−a Review. *Applied Energy* **2019**, *235*, 846−873.
(43) Chen, F.; Wolcott, M. Polyethylene/Paraffin Binary Composites for Phase Change Material Energy Storage in Building: a Morphology, Thermal Properties, and Paraffin Leakage Study. *Sol. Energy Mater. Sol. Cells* **2015**, *137*, 79−85.
(44) Krupa, I.; MikovÁ, G.; Luyt, A. Polypropylene as a Potential Matrix for the Creation of Shape Stabilized Phase Change Materials. *Eur. Polym. J.* **2007**, *43*, 895−907.
(45) Zhang, Q.; Cui, K.; Feng, J.; Fan, J.; Li, L.; Wu, L.; Huang, Q. Investigation on the Recovery Performance of Olefin Block Copolymer/Hexadecane Form Stable Phase Change Materials with Shape Memory Properties. *Sol. Energy Mater. Sol. Cells* **2015**, *132*, 632−639.
(46) Ma, T.; Li, L.; Wang, Q.; Guo, C. High-Performance Flame Retarded Paraffin/Epoxy Resin Form-Stable Phase Change Material. *J. Mater. Sci.* **2019**, *54*, 875−885.
(47) Wu, W.; Wu, W.; Wang, S. Form-Stable And Thermally Induced Flexible Composite Phase Change Material for Thermal Energy Storage and Thermal Management Applications. *Applied Energy* **2019**, *236*, 10−21.
(48) Xiao, M.; Feng, B.; Gong, K. Thermal Performance Of A High Conductive Shape-Stabilized Thermal Storage Material. *Sol. Energy Mater. Sol. Cells* **2001**, *69*, 293−296.
(49) Liu, Z.; Wu, B.; Fu, X.; Yan, P.; Yuan, Y.; Zhou, C.; Lei, J. Two Components Based Polyethylene Glycol/Thermosetting Solid-Solid Phase Change Material Composites as Novel Form Stable Phase Change Materials for Flexible Thermal Energy Storage Application. *Sol. Energy Mater. Sol. Cells* **2017**, *170*, 197−204.
(50) Yuan, K.; Zhou, Y.; Sun, W.; Fang, X.; Zhang, Z. A Polymer-Coated Calcium Chloride Hexahydrate/Expanded Graphite Composite Phase Change Material with Enhanced Thermal Reliability and Good Applicability. *Composites Science and Technology* **2018**, *156*, 78−86.
(51) Qian, Y.; Han, N.; Zhang, Z.; Cao, R.; Tan, L.; Li, W.; Zhang, X. Enhanced Thermal-to-Flexible Phase Change Materials Based on Cellulose/Modified Graphene Composites for Thermal Management of Solar Energy. *ACS Appl. Mater. Interfaces* **2019**, *11*, 45832−45843.
(52) Mu, M.; Basheer, P.; Sha, W.; Bai, Y.; Mcnally, T. Shape Stabilised Phase Change Materials Based on a High Melt Viscosity HDPE and Paraffin Waxes. *Applied Energy* **2016**, *162*, 68−82.
(53) Alkan, C.; GÜNther, E.; Hiebler, S.; Ensari, Ö. F.; Kahraman, D. Polyurethanes as Solid−Solid Phase Change Materials for Thermal Energy Storage. *Solar Energy* **2012**, *86*, 1761−1769.
(54) Xia, Y.; Zhang, H.; Huang, P.; Huang, C.; Xu, F.; Zou, Y.; Chu, H.; Yan, E.; Sun, L. Graphene-Oxide-Induced Lamellar Structures Used to Fabricate Novel Composite Solid-Solid Phase Change Materials for Thermal Energy Storage. *Chem. Eng. J.* **2019**, *362*, 909−920.
(55) Chen, C.; Liu, W.; Wang, Z.; Peng, K.; Pan, W.; Xie, Q. Novel Form Stable Phase Change Materials Based on the Composites of Polyethylene Glycol/Polymeric Solid-Solid Phase Change Material. *Sol. Energy Mater. Sol. Cells* **2015**, *134*, 80−88.
(56) Lu, X.; Fang, C.; Sheng, X.; Zhang, L.; Qu, J. One-Step and Solvent-Free Synthesis of Polyethylene Glycol-Based Polyurethane as Solid−Solid Phase Change Materials for Solar Thermal Energy Storage. *Ind. Eng. Chem. Res.* **2019**, *58*, 3024−3032.
(57) Mu, S.; Guo, J.; Yu, Y.; An, Q.; Zhang, S.; Wang, D.; Chen, S.; Huang, X.; Li, S. Synthesis and Thermal Properties of Cross-Linked Poly(Acrylonitrile-co-Itaconate)/Polyethylene Glycol as Novel Form-Stable Change Material. *Energy Convers. Manage.* **2016**, *110*, 176−183.
(58) Chen, C.; Liu, W.; Yang, H.; Zhao, Y.; Liu, S. Synthesis of Solid−Solid Phase Change Material for Thermal Energy Storage by Crosslinking of Polyethylene Glycol With Poly (Glycidyl Methacrylate). *Solar Energy* **2011**, *85*, 2679−2685.
(59) Xiang, H.; Wang, S.; Wang, R.; Zhou, Z.; Peng, C.; Zhu, M. Synthesis and Characterization of an Environmentally Friendly PHBV/PEG Copolymer Network as a Phase Change Material. *Science China Chemistry* **2013**, *56*, 716−723.
(60) Wang, Y.; Mi, H.; Zheng, Q.; Ma, Z.; Gong, S. Flexible Infrared Responsive Multi-Walled Carbon Nanotube/Form-Stable Phase Change Material Nanocomposites. *ACS Appl. Mater. Interfaces* **2015**, *7*, 21602−21609.
(61) Chen, X.; Gao, H.; Yang, M.; Xing, L.; Dong, W.; Li, A.; Zheng, H.; Wang, G. Smart Integration of Carbon Quantum Dots in Metal-Organic Frameworks for Fluorescence-Functionalized Phase Change Materials. *Energy Storage Materials* **2019**, *18*, 349−355.
(62) Sienkiewicz, A.; Krasucka, P.; Charmas, B.; Stefaniak, W.; Goworek, J. Swelling Effects in Cross-Linked Polymers by Thermogravimetry. *J. Therm. Anal. Calorim.* **2017**, *130*, 85−93.
(63) Richbourg, N. R.; Peppas, N. A. The Swollen Polymer Network Hypothesis: Quantitative Models of Hydrogel Swelling, Stiffness, and Solute Transport. *Prog. Polym. Sci.* **2020**, *105*, 101243.
(64) Zhang, Q.; Feng, J. Difunctional Olefin Block Copolymer/Paraffin Form-Stable Phase Change Materials with Simultaneous Shape Memory Property. *Sol. Energy Mater. Sol. Cells* **2013**, *117*, 259−266.
(65) Dai, W.; Lv, L.; Lu, J.; Hou, H.; Yan, Q.; Alam, F. E.; Li, Y.; Zeng, X.; Yu, J.; Wei, Q.; Xu, X.; Wu, J.; Jiang, N.; Du, S.; Sun, R.; Xu, J.; Wong, C. P.; Lin, C. T. A Paper-Like Inorganic Thermal Interface Material Composed of Hierarchically Structured Graphene/Silicon Carbide Nanorods. *ACS Nano* **2019**, *13*, 1547−1554.
(66) Yang, J.; Tang, L.-S.; Bao, R.-Y.; Bai, L.; Liu, Z.-Y.; Yang, W.; Xie, B.-X.; Yang, M.-B. Largely Enhanced Thermal Conductivity of Poly (Ethylene Glycol)/ Boron Nitride Composite Phase Change Materials for Solar-Thermal-Electric Energy Conversion and Storage With Very Low Content of Graphene Nanoplatelets. *Chem. Eng. J.* **2017**, *315*, 481−490.

Downloaded from pubs.acs.org/aamick/article-pdf/13/49/59364/1279884/aam1c20147.pdf by DOKUZ EYLUL UNIV user on 05 September 2026

https://doi.org/10.1021/acsami.1c20147
ACS Appl. Mater. Interfaces 2021, 13, 59364−59372